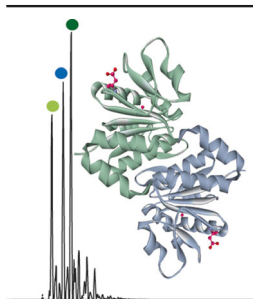# Structural Characterization of Missense Mutations Using High Resolution Mass Spectrometry: A Case Study of the Parkinson's-Related Protein, DJ-1

Gili Ben-Nissan, Almog Chotiner, Mark Tarnavsky, Michal Sharon

Department of Biological Chemistry, Weizmann Institute of Science, Rehovot, 7610001, Israel

Abstract. Missense mutations that lead to the expression of mutant proteins carrying single amino acid substitutions are the cause of numerous diseases. Unlike gene lesions, insertions, deletions, nonsense mutations, or modified RNA splicing, which affect the length of a polypeptide, or determine whether a polypeptide is translated at all, missense mutations exert more subtle effects on protein structure, which are often difficult to evaluate. Here, we took advantage of the spectral resolution afforded by the EMR Orbitrap platform, to generate a mass spectrometry-based approach relying on simultaneous measurements of the wild-type protein and the missense variants. This approach not only considerably shortens the analysis time due to the concurrent acquisition but, more importantly, enables direct comparisons between the wild-type protein and the variants, allowing identification of even subtle structural changes. We demonstrate our approach using the Parkinson's-associated protein, DJ-1. Together with the wild-type protein, we examined two missense mutants, DJ-1$_{A104T}$ and DJ-1$_{D149A}$, which lead to early-onset familial Parkinson's disease. Gas-phase, thermal, and chemical stability assays indicate clear alterations in the conformational stability of the two mutants: the structural stability of DJ-1$_{D149A}$ is reduced, whereas that of DJ-1$_{A104T}$ is enhanced. Overall, we anticipate that the methodology presented here will be applicable to numerous other missense mutants, promoting the structural investigations of multiple variants of the same protein.

Keywords: Native mass spectrometry, Missense mutations, Orbitrap EMR mass spectrometer, DJ-1, Parkinson's disease

Introduction

To date, the application of native mass spectrometry (MS), in which intact protein complexes are transferred into the gas phase, has become routine [1–4]. Numerous examples exist in the literature demonstrating how this structural biology tool is used for defining the stoichiometry, architecture, and topology of protein complexes. In general, the ability to structurally characterize large, heterogenic, and asymmetric protein assemblies, species that are often not amenable to analysis by high-resolution techniques, is the main power of native MS. Successful analyses of such challenging systems have recently been demonstrated through the characterization of mega Dalton species such as viruses [5], heterogeneous ligand bound populations [6], polydisperse assemblies such as αβ-crystallin [7], insoluble amyloid aggregates [8], and even membrane protein complexes [9].

Typically, native MS analysis has been performed using hybrid mass spectrometers, which combine a quadrupole mass filter with an orthogonal time-of-flight (TOF) analyzer [10, 11]. These instruments were specially modified to enable high mass transmission, separation, and detection [10, 11]. Recently, however, analysis of large protein complexes has also become feasible, by means of a modified Orbitrap instrument [12]. Unlike the TOF mass analyzer, which measures flight times, the Orbitrap analyzer measures the axial frequency of oscillation of trapped ions along a central electrode [13]. Similar to TOF-based platforms, the frequency of the front-end ion guides was reduced to improve transmission of high-mass ions, and adjustments were made in the source region to enhance
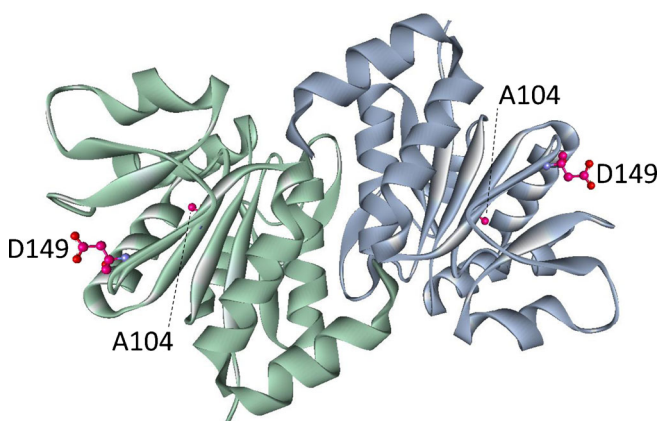
Correspondence to: Michal Sharon; *e-mail:* michal.sharon@weizmann.ac.il

desolvation [12]. Advantages of this modified extended mass range (EMR) Orbitrap instrument include high resolving power, accuracy, and sensitivity [12, 14]. We therefore wished to examine whether this platform could be utilized for structural characterization of missense mutants (i.e., variants of the same protein that differ by a single amino acid substitution [15, 16]). Considering that the wild-type (WT) protein and the missense mutants are very close in mass (mass shifts range between 2 and 129 Da) and are often undistinguishable in structure, their characterization is not trivial. In this study we specifically focused on the characterization of DJ-1 missense mutants.

DJ-1 is a highly conserved homodimer, ubiquitously expressed in cells (for review, see [17, 18]). In general, DJ-1 is known to protect cells from oxidative stress caused by reactive oxygen species, but how this is achieved at the molecular level is unclear. Recently, we discovered that DJ-1 is a regulator of the 20S proteasome [19]. Specifically, we showed that DJ-1 physically binds the 20S proteasome and inhibits its activity, rescuing partially unfolded proteins from degradation. Interestingly, a decade ago, it was realized that missense, truncation, and splice site mutations in DJ-1 all lead to an autosomal recessive, early-onset familial form of Parkinson's disease (PD; reviewed in refs [17, 18, 20]). Whether these modifications affect the structural properties of the protein, and its ability to inhibit the 20S proteasome, is not clear.

Here, we set out to investigate the structural and functional properties of two naturally occurring missense mutants, DJ-1_{A104T} and DJ-1_{D149A} (Figure 1). In particular, we took advantage of the high resolution afforded by the Orbitrap EMR platform to simultaneously examine, within the same needle, a mixture containing the WT protein and the two missense mutational variants, DJ-1_{A104T} and DJ-1_{D149A}, with monomeric molecular masses of 19,760, 19,790, and 19,716 Da, respectively. We measured the gas phase, thermal, and chemical stabilities of the three DJ-1 forms, and correlated this structural information with findings from functional assays. Taken

together, our analysis suggests that a lesser degree of structural stability enhances the functional ability of DJ-1 to inhibit the 20S proteasome. Taking a broader view, and considering the challenges of studying differential structural properties of single-point mutational variants, we anticipate that the approach we present here, which offers direct internal reference of the mutants to the WT protein, will broaden the characterization of other disease-causing missense mutants.

Materials and Methods

Rat liver 20S proteasomes, α-synuclein and the DJ-1 variants were purified as described [19]. Site-directed mutagenesis of the DJ-1 gene was performed using the Q5 Site-Directed Mutagenesis Kit (New England Biolabs, Ipswich, Massachusetts, USA), according to the manufacturer's instructions. For the different stability assays, proteins were buffer exchanged separately into 0.5 M ammonium acetate + 50 mM ethylenediammonium diacetate (EDDA) [5], and their concentrations were then determined, using a Bradford protein quantification assay (Bio-Rad, Hercules., California, USA). Proteins were then diluted to 10 μM in the same buffer, and mixed at a ratio of 1:1:1.

Degradation Assays

Degradation assays were performed as described previously [19]. At different time points, 10 μL aliquots of the degradation reaction were removed and flash-frozen in liquid nitrogen. Samples were then boiled with 5× Laemmli sample buffer and loaded onto a 15% SDS-PAGE gel. Gels were stained with GelCode Blue Stain Reagent (Thermo Fisher Scientific, Massachusetts USA) and scanned. Intensity of the α-synuclein bands was quantified using the ImageJ software (National Institute of health, Bethesda, Maryland, USA). Signal intensities of α-synuclein at the different time points were normalized with respect to their levels at T0 and referred to as 100%, after reduction of background intensity. Each experiment was repeated at least three times; reported values represent an average ± standard deviation.

Native Mass Spectrometry

Nanoelectrospray ionization (nano-ESI) MS experiments were performed on three different instruments: Synapt G1 and G2 instruments (Waters, Hertfordshire, UK) and a Q-Exactive Plus Orbitrap EMR (Thermo Fisher Scientific, Bremen, Germany). All spectra were calibrated externally, using cesium iodide. Spectra obtained from the Synapt instruments are shown with minimal smoothing; no smoothing was done for the Q-Exactive Plus Orbitrap EMR data.

Typically, an aliquot of 2 μL protein solution was loaded into a gold-coated nano-ESI capillary prepared in-house, as previously described [21], and sprayed into the instruments. Conditions within the mass spectrometers were adjusted to preserve noncovalent interactions, with the source operating in positive mode. The following experimental parameters were used: Synapt G1 - capillary voltage of 1.3 kV, sampling cone

Figure 1. Structure of the DJ-1 homodimer. Ribbon diagram of the DJ-1 homodimer, with one monomer colored in green, and the other in light blue. For each monomer, the two mutated residues, A104 and D149, are shown in ball and stick representation, in magenta. The figure was prepared using coordinates from the Protein Data Bank (1UCF) [29]

voltage 17 V, trap DC bias 22 V, extraction cone voltage 0.5 V, trap and transfer collision energies 5 V. Synapt G2 - capillary voltage 1.2 kV, sampling cone voltage 30 V, trap DC bias 22 V, extraction cone voltage 5 V, helium cell gas flow 120 mL/min, trap collision energy 5 V. Both Synapt instruments were operated in ion mobility (IM), and TOF V modes. The Q-Exactive Plus Orbitrap EMR was operated at capillary voltage 1.7 kV, and argon was used as the collision gas in the higher energy collision-induced dissociation (HCD) cell. For analysis of the DJ-1/20S proteasome interaction, MS spectra were recorded at low resolution (5000), and the HCD cell voltage was set to 20–50 V, at trapping gas pressure setting of 3.9. For tandem MS (MS/MS) analyses, a wide isolation window of ±2000 m/z around the most intense charge state of the 20S proteasome (around 12,000 m/z) was set in the quadrupole, allowing the transmission of only high m/z species. Transmitted ions were subjected to collision-induced dissociation in the HCD cell, at an accelerating voltage of 200 V, and the trapping gas pressure was set to 1.5. Stability assays were performed on the Q-Exactive Plus Orbitrap EMR at 17,500 resolution, and the trapping gas pressure was set to 1. Gas-phase stability was monitored at a range of HCD voltages, from 40 to 130 V, whereas thermal and chemical stability assays were measured without applying HCD voltage.

IM-MS measurements were performed on the Synapt G1 instrument. Instrument parameters were as follows: capillary voltage of 1.3 kV, sampling cone - 17 V, extraction cone 0.5 V, trap and transfer collision energies 5 V, trap DC bias – 21.6 V. Nitrogen was used as the IMS gas, at a flow of 24 mL/min, IM wave velocity was set to 200 m/s, and wave height was set to 8 V. Collision cross-sections were calculated for the lowest charge state of the DJ-1 dimers, +11, as described [22]. In brief, four proteins or protein complexes were used for calibration: cytochrome c (12.2 kDa), β-lactoglobulin (37.3 kDa), avidin (64.2 kDa), and concanavalin A (103.1 kDa) (all purchased from Sigma). All calibrants were dissolved in 200 mM ammonium acetate solutions, to retain a native-like conformation. All IM-MS results presented were averaged from three independent experiments. For each experiment, measurements were conducted on the same day; the only parameters modified for the test and calibrating proteins were capillary voltages and backing gas pressure. Theoretical CCSs for human DJ-1 (PDB 1UCF) was calculated using the Driftscope Projection Approximation (PA) algorithm (Waters).

20S Proteasome–DJ-1 Binding Assay

For binding assays, 20 pmol of purified 20S proteasome were mixed with the different DJ-1 variants at a ratio of 1:50 (20S proteasome:DJ-1) and incubated overnight at 4 °C. Prior to native MS analysis, the proteins were buffer exchanged into 150 mM ammonium acetate, and then analyzed in the Q-Exactive Plus Orbitrap EMR.

Gas Phase Stability Assays

The three DJ-1 variants were buffer exchanged into 0.5 M ammonium acetate + 50 mM EDDA, mixed at equimolar ratio (10 μM each), and immediately analyzed by native MS using the Q-Exactive Plus Orbitrap EMR. Spectra were recorded at different HCD cell collision energies, ranging from 40 to 130 V.

Thermal Stability Assays

The three DJ-1 variants were buffer exchanged as described above and mixed at equimolar ratio (10 μM each). Aliquots of 10 μL of the mix were incubated for 3 min at different temperatures, ranging from 45 to 67.5 °C. Samples were then allowed to cool for 3 min at room temperature, and centrifuged at 15,000 g for 5 min at 4 °C, to pellet down aggregates. The supernatant was carefully collected and analyzed by native MS using the Q-Exactive Plus Orbitrap EMR.

Chemical Stability Assays

The three DJ-1 variants were buffer exchanged as described above and mixed at equimolar ratio (10 μM each). Acetonitrile was mixed with the same buffer to make stock solutions of 12.5%–100%. Aliquots of 8 μL protein mix were mixed with 2 μL of the different acetonitrile stock solutions, to make final acetonitrile concentrations of 2.5%–20%. The proteins were then incubated for 3 min at room temperature, and centrifuged at 15,000 g for 5 min, at room temperature, to pellet down aggregates. The supernatant was carefully collected and analyzed by native MS in the Q-Exactive Plus Orbitrap EMR.

### Calculation of Relative Levels of the DJ-1 Variants

The relative abundance of the different DJ-1 variants under any given experimental condition was determined by measuring the peak heights of the different charge states. In the gas phase stability assay, the monomeric DJ-1 variants appeared primarily as a single charge state (+7), whereas in the thermal and chemical stability assays, 2–3 charge states were detected for each DJ-1 dimer variant. Therefore, the total intensity of each variant was calculated as the sum of intensities of its corresponding charge states. In each experiment, the total intensities of all three DJ-1 variants were summed and referenced as 100% intensity; the relative intensity of each variant was considered as a percentage of the total intensity. Each stability assay was performed at least three times.

Results and Discussion

The Ability of DJ-1$_{D149A}$ to Inhibit the 20S Proteasome is Enhanced, in Comparison to DJ-1$_{A104T}$ and the WT Protein

To examine whether DJ-1$_{A104T}$ and DJ-1$_{D149A}$ can protect substrates from 20S proteasome-mediated degradation, as does the WT protein, we performed degradation assays. As a

substrate, we used the intrinsically disordered protein α-synuclein, which is susceptible to 20S proteolysis [19]. The time-dependent degradation assays indicated that α-synuclein is stable in the absence of the 20S proteasome; however, following the addition of highly purified 20S proteasome particles, it is rapidly degraded (Figure 2). The presence of DJ-1$_{WT}$ and DJ-1$_{A104T}$ led to a vast decrease in the degradation rate of α-synuclein. This effect was much more pronounced in the case of DJ-1$_{D149A}$, which was capable of abolishing the proteolysis completely, as indicated by the coinciding degradation kinetics curves of free α-synuclein and α-synuclein, with DJ-1$_{D149A}$ and the 20S
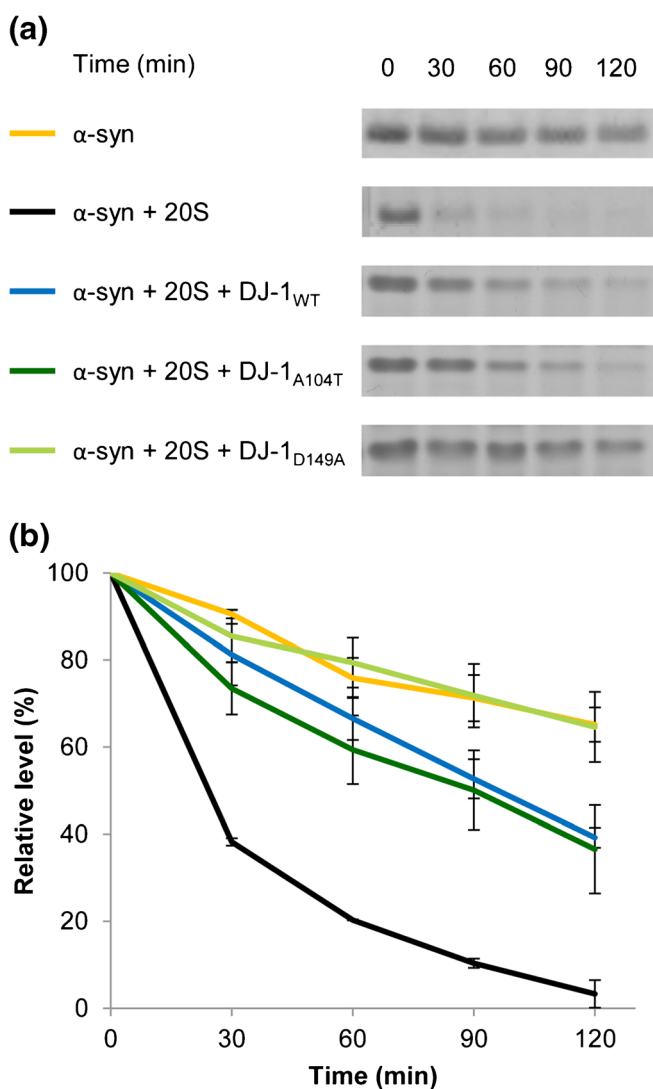
Figure 2. The ability of DJ-1$_{D149A}$ to inhibit the 20S proteasome is improved, in comparison to DJ-1$_{A104T}$ and the WT protein. To examine whether DJ-1$_{A104T}$ and DJ-1$_{D149A}$ can protect substrates from 20S proteasome proteolysis, we performed a series of time-dependent degradation assays, using the intrinsically disordered protein α-synuclein (α-syn) as a substrate. At the indicated time points, aliquots were quenched and evaluated by SDS-PAGE (**a**), followed by quantitative image analysis (**b**). Error bars represent standard deviation of three independent experimental measurements

proteasome. Overall, these results indicate that a single amino acid substitution is capable of modulating DJ-1's functional capability.

DJ-1$_{A104T}$ and DJ-1$_{D149A}$ Mutational Variants Bind the 20S Proteasome Similarly to the Wild-Type Protein

We next wished to examine the propensity of DJ-1$_{A104T}$ and DJ-1$_{D149A}$ to interact with the 20S proteasome. We therefore monitored the physical binding of the proteins by means of native MS. Spectra were recorded after mixing the 20S proteasome with the DJ-1 variants. Free 20S proteasome was used as control (Figure 3 and Supplemental Figure 1). In each of these experiments, the 20S proteasome-associated complexes appeared as charge state series around 12,000 m/z, but the measured peaks were not resolved enough to unambiguously determine whether DJ-1$_{WT}$ or the mutational variants were bound to 20S (Figure 3a, inset). Therefore, tandem MS (MS/MS) experiments were performed in which a region around the major charge state of the complex was isolated in the quadrupole. The isolated ions were subjected to collisional activation in the HCD cell, and the individual subunits, which were stripped from the complex, were identified. The spectrum recorded for the free 20S proteasome gave rise to the dissociation of four α-subunits (Figure 3a), consistent with the architecture of this complex, in which the two α ring structures are exposed [23].

Comparison of this spectrum with that recorded for the 20S proteasome in the presence of the DJ-1 variants revealed additional peaks that correspond in mass to the monomeric DJ-1 variants (Figure 3b–d). By extrapolation, we can therefore conclude that prior to MS/MS analysis, both DJ-1$_{WT}$ and the two missense mutants were bound to the 20S proteasome.

DJ-1$_{A104T}$, DJ-1$_{D149A}$, and the WT Protein Display Similar CCS Values

To understand whether the enhanced functionality of the DJ-1$_{D149A}$ variant results from changes in the protein compactness, we carried out ion mobility MS (IM-MS) measurements. In these experiments, the ions travel under the influence of a weak electric field, and are separated based on their velocity within a chamber pressurized with inert neutral gas. Larger ions collide more frequently with the neutral gas, hindering their progress and therefore increasing their 'drift time', relative to more compact ions [24]. Drift times are converted to collision cross-sections (CCS), which provide information on the overall size and conformation of the ions [25, 26]. A CCS value of about 2500 Å^2 was determined experimentally for all DJ-1 variants. Theoretical CCS for the human DJ-1 yielded a value of 2388 Å^2, in agreement with the measured CCS value (Figure 4a). Moreover, corresponding two-dimensional MS spectra illustrate that like the WT protein, DJ-1$_{A104T}$ and DJ-1$_{D149A}$ adopt a homodimeric topology with a charge state distribution similar to that of the WT protein (Figure 4b–d). As expected, monomeric forms of DJ-1 were not detected. Overall, these observations suggest that the structural compactness of DJ-1$_{A104T}$ and DJ-1$_{D149A}$ is similar to that of the WT protein and that within the limits of the ion mobility experiment, they cannot be distinguished.
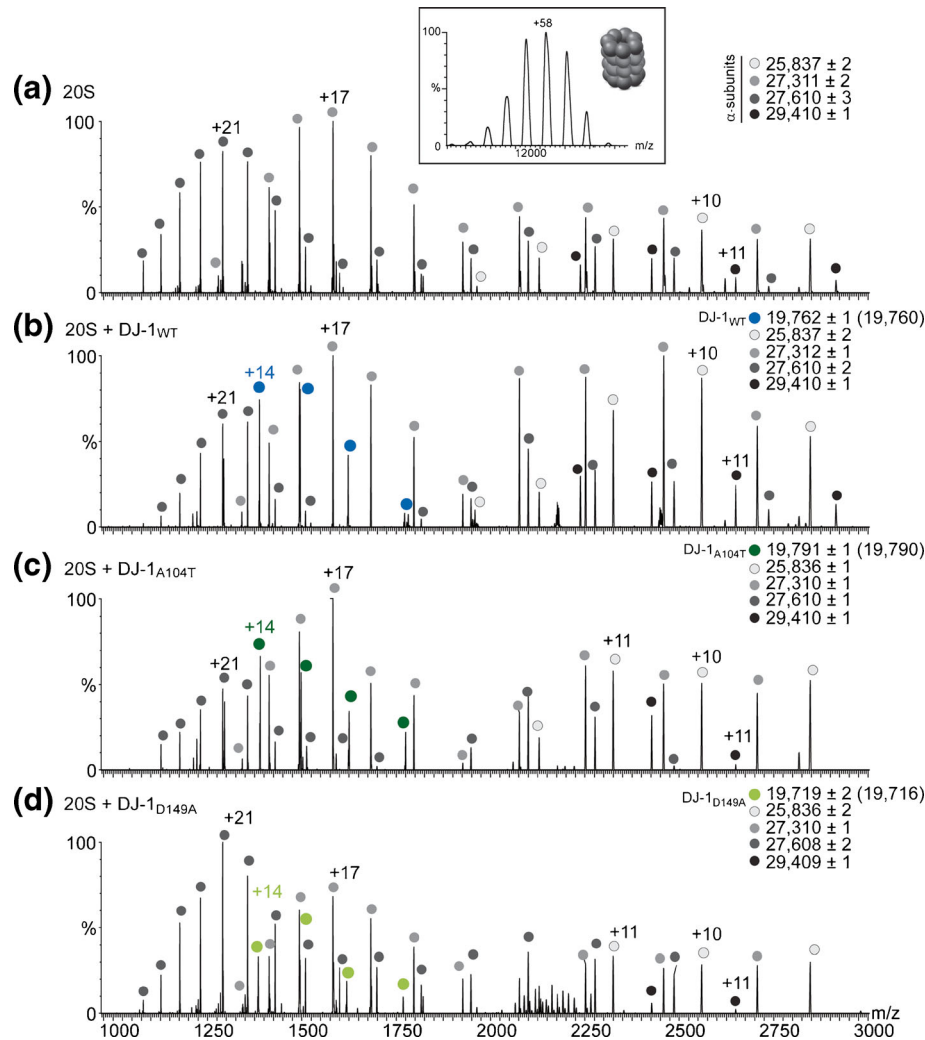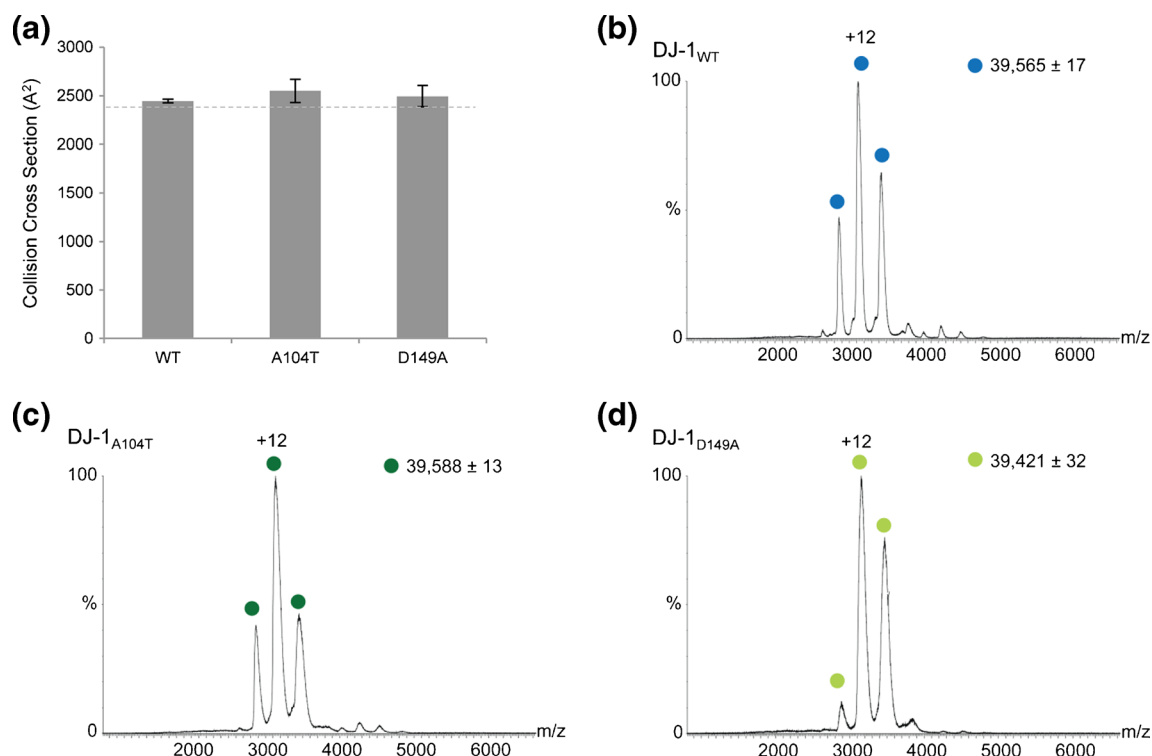
Figure 3. DJ-1 and its mutational variants physically bind to the 20S proteasome. The 20S proteasome was incubated alone (**a**), or together with the different DJ-1 variants (**b**)–(**d**) overnight at 4 °C, and then subjected to native MS analysis using the Q Exactive Plus Orbitrap EMR. For each sample, the most intense charge states of the 20S proteasome were +58 and +59, around 12,000 *m/z*. Ions around 12,000 ± 2000 *m/z* were isolated and subjected to MS/MS analysis. Inset in (**a**) shows a representative MS spectrum of the 20S proteasome. Spectra in (**a**)–(**d**) focus on the lower range of the *m/z* spectrum, following MS/MS, where single α-subunits that were stripped off the 20S proteasome complex, appear. Spectrum in (**a**) shows the dissociation of four different alpha subunits from the 20S proteasome complex (labeled by various shades of grey-black circles). In comparison, spectra recorded for the 20S proteasome in the presence of the different DJ-1 variants (**b**)–(**d**), reveal an additional charge state series, corresponding in mass to the monomeric forms of the DJ-1 variants (labeled by colored circles). Theoretical masses of monomeric DJ-1 variants without the initial methionine are in brackets. By extrapolation, we can therefore conclude that prior to MS/MS analysis, the three DJ-1 variants were bound to the 20S proteasome

A Mixture of DJ-1 Missense Mutants and Wild-Type Protein Can Be Highly Resolved by Native MS

To detect whether subtle structural changes are the cause for the differential activity of the DJ-1 variants, we wished to examine all proteins concurrently. Specifically, we aimed to create a set-up that would enable us to mix the three DJ-1 variants and spray them together from the same needle, allowing all variants to experience exactly the same experimental conditions. Notably, DJ-1$_{A104T}$ and DJ-1$_{D149A}$ differ from the monomeric WT protein by only +44 and –30 Da, respectively. We therefore screened for MS conditions that would allow us to achieve highly resolved peaks, reflecting the small differences in mass between the DJ-1 variants.

Initially, we examined different buffer conditions, using three different mass spectrometers; Synapt G1, Synapt G2, and Orbitrap EMR. We found that an equimolar mix of the three DJ-1 variants in buffer containing 0.5 M ammonium acetate and 50 mM EDDA [6], analyzed on the Orbitrap EMR, generated a well-resolved spectrum of the dimeric DJ-1 proteins, enabling us to distinguish between the three variants. In contrast, analysis of the same sample on both Synapt instruments did not yield the required resolution (Figure 5). We therefore continued the stability analyses on the Orbitrap EMR platform, simultaneously recording spectra of the three DJ-1 variants. Under the experimental conditions we used, subunit

Figure 4. DJ-1$_{WT}$ and its missense mutants display a similar fold. DJ-1$_{WT}$ and its mutational variants DJ-1$_{A104T}$ and DJ-1$_{D149A}$ were subjected to IM-MS analysis on a Synapt G1 instrument, and their collision cross-sections were calculated (**a**). The horizontal gray line designates the theoretical CCS value calculated using the PA method for the WT protein crystal structure. Error bars represent standard deviation of three independent experimental measurements. (**b**)–(**d**) Representative two-dimensional spectra of the three DJ-1 variants emphasize that like the WT protein, the mutants adopt a homodimeric structure and display a similar charge state distribution. Taken together, the results show that all three proteins possess similar structural compactness

exchange was not observed after mixing the three DJ-1 variants, even after prolonged incubation times. Overall, we anticipate that simultaneous analysis of the different proteins eliminates the effects of needle positioning and needle–needle variations that influence the measurements [27]. In addition, it enables the use of the WT protein as an internal reference.

DJ-1$_{A104T}$ and DJ-1$_{D149A}$ Exhibit Altered Stability, in Comparison to the Wild-Type Protein

Initially, we determined the relative gas-phase stability of the three DJ-1 forms, sprayed as an equimolar mixture. To this end, we subjected the ions to collision-induced dissociation by increasing the collision energy (CE) voltage in a stepwise manner, from 40 to 130 V. The amount of DJ-1 monomers that are dissociated from the homodimeric complex were then probed, and their relative intensity calculated (Figure 6a). The results indicate that while the substitution of aspartic acid 149 with alanine reduces the intermolecular stability of DJ-1 in comparison to the WT protein, the replacement of alanine 104 with threonine stabilizes it. Overall, it can be seen that single point mutations can differentially alter the structural stability of the protein.

To further assess the relative stability of the DJ-1 variants, we compared the thermal stability of the proteins. The three DJ-1 variants were mixed and incubated at increasing temperatures

ranging from 45 to 67.5 °C, for 3 min. Following centrifugation to remove aggregates, mass measurements were performed. In all spectra, we obtained only dimeric species: although their charge state distribution remained constant along the entire temperature gradient, their relative abundance differed. This observation suggests that the MS data reflect the quantity of intact DJ-1 proteins that remain soluble in solution. The relative abundance of the DJ-1 protein variants was then quantified by normalizing the peak height intensity of the dimers' charge states. The results demonstrate that at temperatures up to 60 °C, DJ-1$_{A104T}$ exhibits higher thermostability in comparison to DJ-1$_{WT}$, whereas DJ-1$_{D149A}$ displays significantly less resistance to heat, relative to the WT protein (Figure 6b). These results are in accordance with the data we obtained from the gas-phase stability assay.

Finally, we assessed the chemical stability of the three DJ-1 variants: proteins were exposed to increasing concentrations of the chaotropic organic solvent acetonitrile, and the relative abundance of the dimeric states of the three DJ-1 variants was measured. The three DJ-1 variants were mixed and incubated with increasing concentrations of acetonitrile, for 3 min. The proteins were then centrifuged to remove aggregates, and the relative abundance of the different dimeric variants was analyzed by native MS measurements. The results corroborated those obtained in the other stability assays: DJ-1$_{A104T}$ displays higher resistance to acetonitrile, whereas DJ-1$_{D149A}$ displays
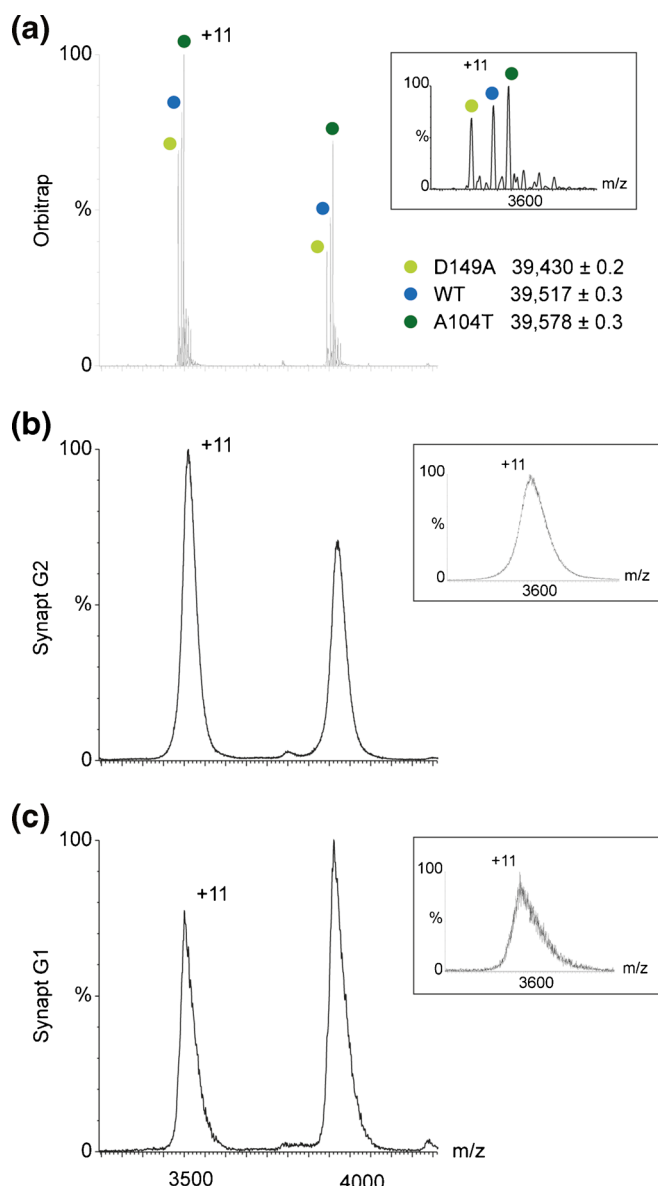
Figure 5. The Q-Exactive plus Orbitrap EMR mass spectrometer produces highly resolved spectra which distinguish between the three DJ-1 variants. The three variants of DJ-1 were buffer exchanged into 0.5 M ammonium acetate + 50 mM EDDA, and mixed at equimolar ratios. Mixtures were analyzed in three different instruments: Q-Exactive plus Orbitrap EMR (**a**), Synapt G2 (**b**), and Synapt G1 (**c**). Analysis in the Orbitrap EMR generated a well-resolved spectrum of the dimeric DJ-1 proteins, and allowed for clear separation between their signals, whereas analysis in the two Synapt instruments generated broad and unresolved peaks. Insets show the enlargement of a single charge state of each series. Measured masses of the three DJ-1 variants are indicated

lower resistance to such chemical denaturation compared with the wild-type protein (Figure 6c).

Taken together, the three different types of stability assays indicated that the two missense mutants were influenced in opposing ways by the amino acid substitution. In comparison to the WT protein, the stability of DJ-1$_{D149A}$ was reduced,
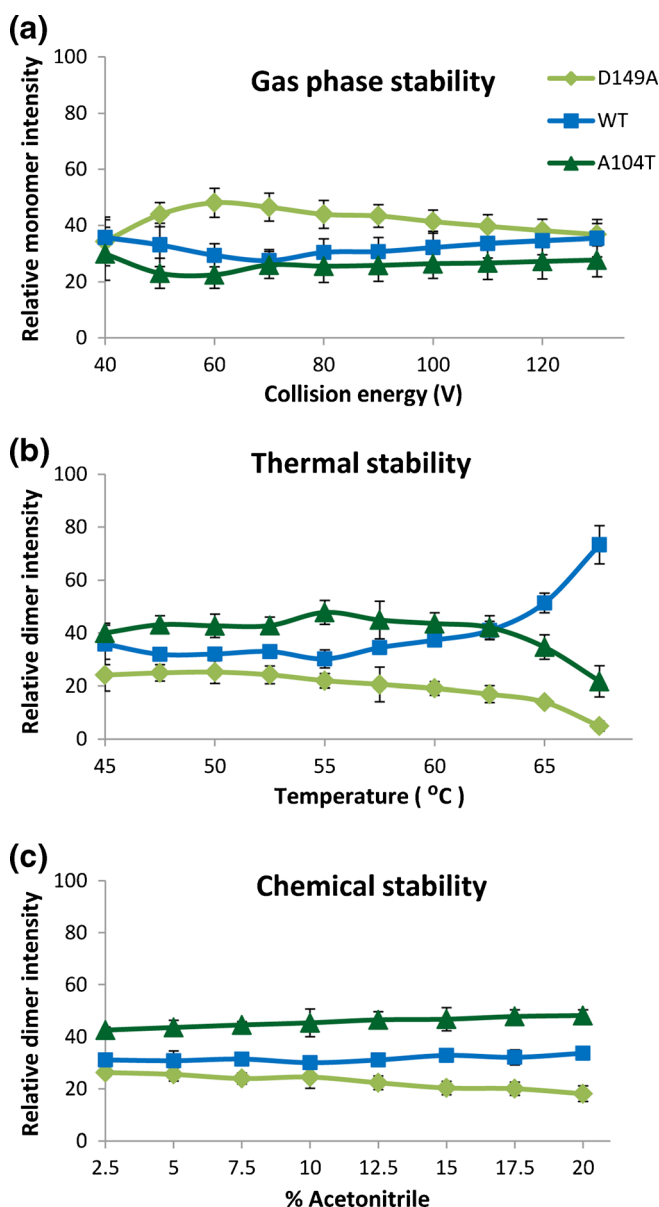
Figure 6. The stability of DJ-1$_{A104T}$ and DJ-1$_{D149A}$ mutational variants differs from that of the wild-type protein. (**a**) An equimolar mix of the three DJ-1 variants was subjected to a gradual elevation of collision energy voltage in a step-wise manner, ranging from 40 to 130 V. Relative intensities of the generated monomers were extracted and plotted. (**b**) A 1:1:1 mixture of the three DJ-1 variants was incubated at increasing temperatures, and then subjected to native MS analysis. The relative intensities of the dimer proteins were extracted and plotted. (**c**) To evaluate the chemical stabilities of the DJ-1 variants, their mix was incubated at elevated concentrations of acetonitrile and then subjected to native MS analysis. The relative intensities of the dimer proteins were calculated and plotted. Error bars represent standard deviation of at least four experiments. Overall, the results show that compared with the WT protein, DJ-1$_{A104T}$ exhibits increased structural stability, whereas DJ-1$_{D149A}$ displays less resistance to the tested experimental conditions

whereas that of DJ-1$_{A104T}$ was increased. As shown in Figure 1, neither of the mutations was located near the subunits interface; therefore, it is unlikely that perturbations in the dimeric interaction constituted the underlying differential character of the mutants. Alterations in the hydrogen bond network, however, could provide an explanation for our results. The D149 side chain forms a hydrogen bond with the K122 backbone; D149 backbone forms a hydrogen bond with the I152 backbone. Each of the K122, D149, and I152 residues is located on a different β-strand, and the hydrogen bond pairing through D149 attains the tertiary fold (Supplemental Figure 2a). Thus, loss of this hydrogen bond network through the substitution of aspartic acid with alanine will disrupt the hydrogen bond interaction with K122 and is likely to induce destabilization, in accord with our observations.

A104 backbone atoms also form two hydrogen bonds with L153 and S155. Both of them, however, are with backbone atoms and within the same β-strand (Supplemental Figure 2b). It is reasonable to speculate that the substitution of alanine with threonine, which introduces a hydroxyl group capable of forming hydrogen bonds, would increase the number of interactions and, consequently, enhance structural stabilizations, as we observed. Overall, it appears that the hydrogen bonding characteristics of DJ-1$_{A104T}$ and DJ-1$_{D149A}$ and the experimental data correlate nicely, supporting the applicability of the simultaneous measurement approach.

Conclusions

Gas phase, thermal and chemical stability assays performed in this study indicate that compared to the WT protein, DJ-1$_{A104T}$ adopts a more stable structure, while the structural stability of DJ-1$_{D149A}$ is reduced. Considering that DJ-1$_{D149A}$ is more capable of inhibiting the 20S proteasome, in comparison to both DJ-1$_{A104T}$ and DJ-1$_{WT}$, these observations may suggest that following its association with the 20S proteasome, DJ-1 undergoes structural rearrangements that enable its inhibitory function. The more relaxed structure of DJ-1$_{D149A}$ may more readily promote such a structural transition.

On a broader view it should be noted that to date more than 67,000 missense mutations have been identified in the human genome (Human Gene Mutation Database, HGMD; http://www.hgmd.org). These mutations are related to many pathological conditions, and are known to influence individual susceptibility to disease and drug treatment [15]. For example, it is known that inactivation of the tumor suppressor p53 by missense mutations is the most frequent genetic alteration in human cancers [28]. Similarly, many neurodegenerative diseases such as Alzheimer's, Parkinson's and Creutzfeldt-Jakob diseases, are also associated with missense mutations [15]. Thus, it is critical to understand the structural impact of such mutations on the target protein, in order to develop therapeutic strategies for pharmacological rescue. Yet single amino acid substitutions may not result in obvious structural changes; on the contrary, in many cases, disease states are associated not

with fold alterations but with a change in the conformational flexibility of the corresponding protein [15]. Over the years, a variety of algorithms have been developed to evaluate the structural effects of such single amino acid substitutions. However, gleaning conclusive insights from such formulas is not always trivial, as we demonstrate for DJ-1$_{A104T}$ and DJ-1$_{D149A}$ using five different algorithms (Supplementary Table 1). Therefore, we anticipate that the method we present here, which enables simultaneous analysis of mutational variants with the WT protein, will promote structural investigations of missense mutants. Such simultaneous measurement not only speeds up the analysis, but also provides a direct internal reference to the WT protein, enabling the identification of subtle structural changes.

Acknowledgments

References

1. Marcoux, J., Robinson, C.V.: Twenty years of gas-phase structural biology. Structure 21, 1541–1550 (2013)
2. Sharon, M.: Biochemistry. Structural MS pulls its weight. Science 340, 1059–1060 (2013)
3. Kaddis, C.S., Loo, J.A.: Native protein MS and ion mobility large flying proteins with ESI. Anal. Chem. 79, 1778–1784 (2007)
4. Snijder, J., Heck, A.J.: Analytical approaches for size and mass analysis of large protein assemblies. Annu. Rev. Anal. Chem. 7, 43–64 (2014)
5. Uetrecht, C., Heck, A.J.: Modern biomolecular mass spectrometry and its role in studying virus structure, dynamics, and assembly. Angew. Chem. Int. Ed. Engl. 50, 8248–8262 (2011)
6. Dyachenko, A., Gruber, R., Shimon, L., Horovitz, A., Sharon, M.: Allosteric mechanisms can be distinguished using structural mass spectrometry. Proc. Natl. Acad. Sci. U. S. A. 110, 7235–7239 (2013)
7. Hochberg, G.K., Benesch, J.L.: Dynamical structure of alphaB-crystallin. Prog. Biophys. Mol. Biol. 115, 11–20 (2014)
8. Woods, L.A., Radford, S.E., Ashcroft, A.E.: Advances in ion mobility spectrometry-mass spectrometry reveal key insights into amyloid assembly. Biochim. Biophys. Acta. 1834, 1257–1268 (2013)
9. Barrera, N.P., Robinson, C.V.: Advances in the mass spectrometry of membrane proteins: from individual proteins to intact complexes. Annu. Rev. Biochem. 80, 247–271 (2011)
10. Sobott, F., Hernandez, H., McCammon, M.G., Tito, M.A., Robinson, C.V.: A tandem mass spectrometer for improved transmission and analysis of large macromolecular assemblies. Anal. Chem. 74, 1402–1407 (2002)
11. Chernushevich, I.V., Thomson, B.A.: Collisional cooling of large ions in electrospray mass spectrometry. Anal. Chem. 76, 1754–1760 (2004)
12. Rose, R.J., Damoc, E., Denisov, E., Makarov, A., Heck, A.J.: High-sensitivity Orbitrap mass analysis of intact macromolecular assemblies. Nat. Methods 9, 1084–1086 (2012)
13. Makarov, A.: Electrostatic axially harmonic orbital trapping: a high-performance technique of mass analysis. Anal. Chem. 72, 1156–1162 (2000)
14. Rosati, S., Rose, R.J., Thompson, N.J., van Duijn, E., Damoc, E., Denisov, E., Makarov, A., Heck, A.J.: Exploring an orbitrap analyzer for the characterization of intact antibodies by native mass spectrometry. Angew Chem. Int. Ed. Engl. 51, 12992–12996 (2012)

15. Stefl, S., Nishi, H., Petukh, M., Panchenko, A.R., Alexov, E.: Molecular mechanisms of disease-causing missense mutations. J. Mol. Biol. **425**, 3919–3936 (2013)

16. Thusberg, J., Vihinen, M.: Pathogenic or not? And if so, then how? Studying the effects of missense mutations using bioinformatics methods. Hum. Mutat. **30**, 703–714 (2009)

17. Kahle, P.J., Waak, J., Gasser, T.: DJ-1 and prevention of oxidative stress in Parkinson's disease and other age-related disorders. Free Radic. Biol. Med. **47**, 1354–1361 (2009)

18. Wilson, M.A.: The role of cysteine oxidation in DJ-1 function and dysfunction. Antioxid. Redox Signal **15**, 111–122 (2011)

19. Moscovitz, O., Ben-Nissan, G., Fainer, I., Pollack, D., Mizrachi, L., Sharon, M.: The Parkinson's-associated protein DJ-1 regulates the 20S proteasome. Nat. Commun. **6**, 6609 (2015)

20. Cookson, M.R.: Parkinsonism due to mutations in PINK1, parkin, and DJ-1 and oxidative stress and mitochondrial pathways. Cold Spring Harb. Perspect Med. **2**, a009415 (2012)

21. Kirshenbaum, N., Michaelevski, I., Sharon, M.: Analyzing large protein complexes by structural mass spectrometry. J. Vis. Exp. (2010). doi:10.3791/19545

22. Bush, M.F., Hall, Z., Giles, K., Hoyes, J., Robinson, C.V., Ruotolo, B.T.: Collision cross sections of proteins and their complexes: a calibration framework and database for gas-phase structural biology. Anal. Chem. **82**, 9557–9565 (2010)

23. Hershko, A., Ciechanover, A.: The ubiquitin system. Annu. Rev. Biochem. **67**, 425–479 (1998)

24. Mason, E.A., McDaniel, E.W. New York : John Wiley and Sons, (1988)

25. Michaelevski, M., Kirshenbaum, N., Sharon, S.: T-wave ion mobility-mass spectrometry: Basic experimental procedures for protein complex analysis. J. Vis. Exp. (2010). doi:10.3791/1985

26. Ruotolo, B.T., Benesch, J.L., Sandercock, A.M., Hyung, S.J., Robinson, C.V.: Ion mobility-mass spectrometry analysis of large protein complexes. Nat. Protoc. **3**, 1139–1152 (2008)

27. El-Faramawy, A., Siu, K.W., Thomson, B.A.: Efficiency of nano-electrospray ionization. J. Am. Soc. Mass. Spectrom. **16**, 1702–1707 (2005)

28. Kato, S., Han, S.Y., Liu, W., Otsuka, K., Shibata, H., Kanamaru, R., Ishioka, C.: Understanding the function-structure and function-mutation relationships of p53 tumor suppressor protein by high-resolution missense mutation analysis. Proc. Natl. Acad. Sci. U. S. A. **100**, 8424–8429 (2003)

29. Honbou, K., Suzuki, N.N., Horiuchi, M., Niki, T., Taira, T., Ariga, H., Inagaki, F.: The crystal structure of DJ-1, a protein related to male fertility and Parkinson's disease. J. Biol. Chem. **278**, 31380–31384 (2003)